J Appl Electrochem (2007) 37:1107–1117
DOI 10.1007/s10800-007-9371-8

ORIGINAL PAPER

Development of a continuous reactor for the electro-reduction of carbon dioxide to formate – Part 2: Scale-up

Hui Li · Colin Oloman

Received: 9 October 2006 / Revised: 15 June 2007 / Accepted: 9 July 2007 / Published online: 28 July 2007

Abstract This paper reports experimental and modeling work for the laboratory scale-up of continuous "trickle-bed" reactors for the electro-reduction of CO_2 to potassium formate. Two reactors (A and B) were employed, with particulate tin 3D cathodes of superficial areas, respectively, 45×10^{-4} (2–14 A) and 320×10^{-4} m^2 (20–100 A). Experiments in Reactor A using granulated tin cathodes (99.9 wt% Sn) and a feed gas of 100% CO_2 showed slightly better performance than that of the tinned-copper mesh cathodes of our previous communications, while giving substantially improved temporal stability (200 vs. 20 min). The seven-fold scaled-up Reactor B used a feed gas of 100% CO_2 with the aqueous catholyte and anolyte, respectively [0.5 M $KHCO_3$ + 2 M KCl] and 2 M KOH, at inlet pressure from 350 to 600 kPa(abs) and outlet temperature 295 to 325 K. For a superficial current density of 0.6–3.1 kA m^{-2} Reactor B achieved corresponding formate current efficiencies of 91–63%, with the same range of reactor voltage as that in Reactor A (2.7–4.3 V), which reflects the success of the scale-up in this work. Up to 1 M formate was obtained in the catholyte product from a single pass in Reactor B, but when the catholyte feed was spiked with 2–3 M potassium formate there was a large drop in current efficiency due to formate cross-over through the Nafion 117 membrane. An extended reactor (cathode) model that used four fitted kinetic parameters and assumed zero formate cross-over was able to mirror the reactor performance with reasonable fidelity over a wide range of conditions (maximum error in formate CE = ±20%), including formate product concentrations up to 1 M.

Keywords Carbon dioxide · Continuous reactor · Electro-reduction · Formate · 3D electrode · Scale-up · Tin granule cathode

Nomenclature

a_1,a_2	Tafel constant for reaction 1, 2 (V)
b_1,b_2	Tafel slope for reaction 1, 2 (V decade^{-1})
C	Concentration of KCl (M)
CE	Current efficiency (–)
$d_{\text{p, average}}$	Average particle diameter (m)
$E_{a,1}$, $E_{a,2}$	Activation energies for reactions 1 and 2 (kJ kmol^{-1})
E_{cell}	Full-cell operating voltage (absolute value) (V)
E_1, E_2	Electrode potential for reaction 1 and 2 (V(SHE))
$E_{r,1}$, $E_{r,2}$	Reversible electrode potential for reaction 1 and 2 (V(SHE))
G	Gas flow rate (mL STP min^{-1})
H	Height of 3D cathode (m)
I	Current (kA)
$i_{o,1}$, $i_{o,2}$	Exchange current densities for reactions 1 and 2 (kA m^{-2})
j_1,j_2	Partial real current density for reaction 1, 2 (kA m^{-2})
j_{1L}	CO_2 mass transfer limited current density for reaction 1 (kA m^{-2})
k_1, k_2	Electrochemical rate constants for reactions 1 and 2 (m s^{-1})
L	Catholyte liquid flow rate (mL min^{-1})
P_{cathode}	Cathode side pressure (kPa(abs))

H. Li · C. Oloman (✉)
Department of Chemical and Biological Engineering, University of British Columbia, Vancouver, BC, Canada, V6T 1Z3
e-mail: coloman@intergate.ca

T	Temperature (K)
W	Width of 3D cathode (m)
α	Electro-chemical charge transfer coefficient (–)
η_1, η_2	Over-potential for reaction 1, 2 (V)
τ	Thickness of 3D cathode (m)

1 Introduction

From recent reviews on the electro-reduction of CO_2 [1, 2] and their associated literature sources, it is evident that a lot of R&D is needed to bring the electro-reduction of CO_2 (ERC) to formate/formic acid into practical application. This R&D embraces stepping from the small batch cells of prior work to a continuous reactor that operates over several thousand hours at practical current density and efficiency (e.g. superficial current density >1 kA m^{-2} and current efficiency >50%), followed by scaling-up to a multi-cell "industrial" reactor in an economically viable continuous electro-chemical process.

Our previous communications [3, 4] report work on the electro-reduction of CO_2 to formate in a laboratory bench-scale single-cell continuous reactor with a cation membrane separator and "trickle-bed" 3D cathode 30 mm wide by 150 mm high (i.e. 45×10^{-4} m^2), designated presently as Reactor A. That work used tinned-copper mesh cathodes in factorial and parametric experiments to capture the effects of eight variables (cathode specific surface, cathode thickness, CO_2 pressure, current density, catholyte conductivity, catholyte species, temperature and time) on reactor performance. The results indicated good prospects for the development of an industrial scale reactor for electro-reduction of carbon dioxide based on the stoichiometry of reactions I, II and IV. However, the cathodes used there exhibited poor catalytic stability (deteriorating after about 20-min operation), due to the loss of tin from the mesh surface.

E^0 V(SHE) @ 298 K, pH 14

Cathode primary: $CO_2(aq) + H_2O + 2e^- \rightarrow HCOO^- + OH^-$ -1.02 (1)

Cathode secondary: $2H_2O + 2e^- \rightarrow H_2 + 2OH^-$ -0.83 (II)

Cathode tertiary: $CO_2 + H_2O + 2e^- \rightarrow CO + 2OH^-$ -0.94 (III)

Anode: $1/2O_2 + H_2O + 2e^- \leftarrow 2OH^-$ $+0.40$ (IV)

Now we report further experimental work, coupled with reactor modeling, as a step toward scaling-up the trickle-bed ERC reactor to industrial capacity. The first objective here was to find a 3D cathode material with longer operating life than tinned-copper mesh—with the prospect of extending the cathode life to several thousand hours. The subsequent work included experiments aimed to reinforce the reactor model and achieve a seven-fold scale-up in the geometric cathode area in a continuous ERC reactor, designated here as Reactor B.

2 Experimental design, apparatus and methods

The work reported here involved factorial, fractional factorial and parametric experiments with two single-cell continuous electrochemical reactors, designated as Reactor A (small) and a scaled-up Reactor B (large). The reactor configuration and process flowsheet are the same as those described in our previous communications [3, 4]. Both reactors use cation membrane separators with 3D cathodes, operating in the continuous flow-by "trickle-bed" mode [5] with co-current upward 2-phase flow of the catholyte liquid and CO_2 gas. Dimensions and operating ranges of Reactors A and B for the present work are summarized below in Table 1 and Figs. 1 and 2.

The experimental work was supported by the reactor (cathode) model, extended from our previous work [3] and summarized here in the Appendix, which helped to interpret the data and predict conditions for the scale-up. No measurements were made of electrode potentials, current distribution or process conditions inside the reactors.

2.1 Cathode material

Several materials were considered to replace the short-lived tinned-copper mesh cathode used in our previous experiments [6]. The most effective of the tested materials were the tin particulates whose properties are listed in Table 2.

As purchased, the tin shot had nearly mono-disperse size distribution and uniform spherical shape. The tin granules, on the other hand, had wide size distribution and irregular shape. In addition, these tin granules were purchased in two separate batches with ostensibly the same specification (SN-131) but with different color, size and shape distribution, as indicated in Table 2. These materials were studied with Reactor A, in which the tinned-copper mesh of our previous work was replaced by a fixed-bed of tin particles contained by a 3.2 mm thick Neoprene gasket (Fig. 1). The cathode feeder was tin foil supported on a copper plate.

Prior to use, fresh or used tin particles were pretreated sequentially with dilute hydrochloric acid (1 M) and potassium hydroxide (1 M) at room temperature

Table 1 Dimensions and operating ranges of Reactors A and B

Condition	Units	Reactor A (small)	Reactor B (large)
Number of cells	–	1	1
Cathode material	–	Tin shot (2.4 mm) Tin granules Batch 1[a] Tin granules Batch 2[a]	Tin granules Batch 2[a]
Cathode dimensions	mm	$H = 150$, $W = 32$, $\tau = 3.2$	$H = 680$, $W = 50$, $\tau = 3.2$
Cathode superficial area	m^2	45×10^{-4}	320×10^{-4}
Catholyte feed (aqueous)	–	0.45 M $KHCO_3$ + 0.5 to 2 M KCl	0.45 M $KHCO_3$ + 2 M KCl + 0 to 3 M $KHCO_2$
Catholyte feed flow	mL/min	10–20	20
Cathode gas (CO_2) feed flow	mL STP/min	400–1600	1600–2200
Anode		316 SS, 10# screen	316 SS, 10# screen
Anolyte	mL/min	1 M KOH, 40 mL/min	2 M KOH, 60 mL/min
Separator	–	Nafion 117	Nafion 117
Cathode pressure (in/out)	kPa(abs)	(140–280)/100	(380–690)/100
Cathode temperature (in/out)	K	(288–296)/(293–323)	(288–296)/(293–323)
Current	A	2–14	20–100
Superficial current density	$kA\ m^{-2}$	0.4–3.1	0.6–3.1
Voltage ($-E_{cell}$)	V	2.01–4.36	2.70–4.45

H = height, W = width, τ = thickness

[a] See Table 2

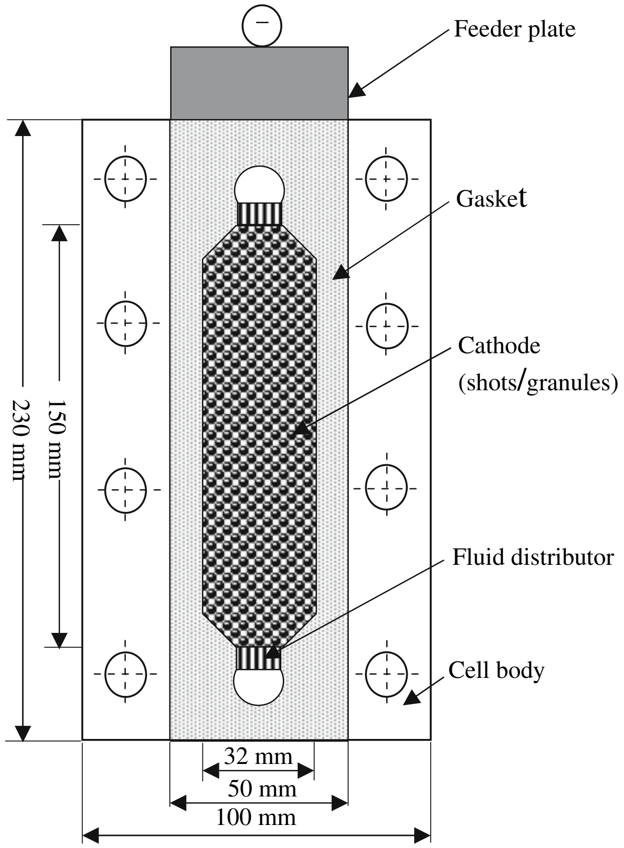

Fig. 1 Front view and dimensions of the cathode compartment of Reactor A

(2–10 min) to strip away the oxide layer and roughen the surface, followed by rinsing with copious de-ionized water. In earlier experiments a pretreatment with 5 wt% nitric acid was shown to be problematic, as it caused a form of tin corrosion that promoted the generation of black/grey tin oxide/hydroxide suspensions in the catholyte during reactor operation [6].

2.2 Reactor A

The configuration and size of Reactor A are essentially those described previously [3, 4] except that the tinned-copper mesh cathode is replaced by a fixed-bed of tin particles. This reactor was operated under a range of conditions to test the cathode stability and to explore the effects of six major process variables on the reactor performance.

2.3 Reactor B

Reactor B is a seven-fold scale-up from Reactor A. As practiced in any scale-up study of an electrochemical reactor [7], the scale-up in the present work took into account of several similarities between the "small" and "large" reactors, including geometric, kinematic and thermal similarities as well as the more important electrical similarity. Electrical similarity was attempted in the present work by employing the same inter-electrode gap and same 3D electrode thickness

Table 2 Characterization of tin shot and granules

Tin particles	Source	Nominal purity wt% Sn	Impurity Sb As Cu Fe, wt%	Voidage (%)	Average diameter (mm)	Specific area (m^2 m^{-3})	Shape factor
Shot	AEE SN 133	99.99	0.04	40	2.39	1500	1
Batch 1 granules	AEE SN 131	99.9	0.15	38	0.379	11000	0.89
Batch 2 granules	AEE SN 131	99.9	0.15	48	0.252	17000	0.59

AEE = Atlantic Equipment Engineers. USA

for the “small “ and the “large “ reactors, aiming to maintain similar potential and current density distributions for the two reactors. The gas loading in Reactor B was not a direct scale-up from that in Reactor A, but was based instead on the stoichiometric requirements for CO_2, with a maximum of 75% CO_2 conversion per pass.

Tin granules were chosen as the cathode for the scale-up due to their high formate current efficiency and stability relative to other materials tested. Figure 2 shows the front view and dimensions of the cathode compartment and Fig. 3 presents the arrangement of the components of Reactor B. On the cathode side, the gasket containing the cathode bed was made with trianglular baffles to re-direct the flow toward the center of the cathode and thus suppress the by-pass of the catholyte along the edges of the bed. On the anode side, a stainless steel mesh ($10^{\#}$) was employed together with a stainless steel plate to improve the current distribution and lower the reactor voltage. The anode and cathode chamber were separated by a Nafion 117 membrane supported on the anode side by a PVC screen, which also acted as a spacer to prevent a possible electrical short between anode and cathode. The reactor assembly was uniformly compressed with 24, 3/8 inch (9 mm) bolts using a torque wrench at about 27 Nm. The dimensions and operating ranges of both Reactors A and B are given in Table 1.

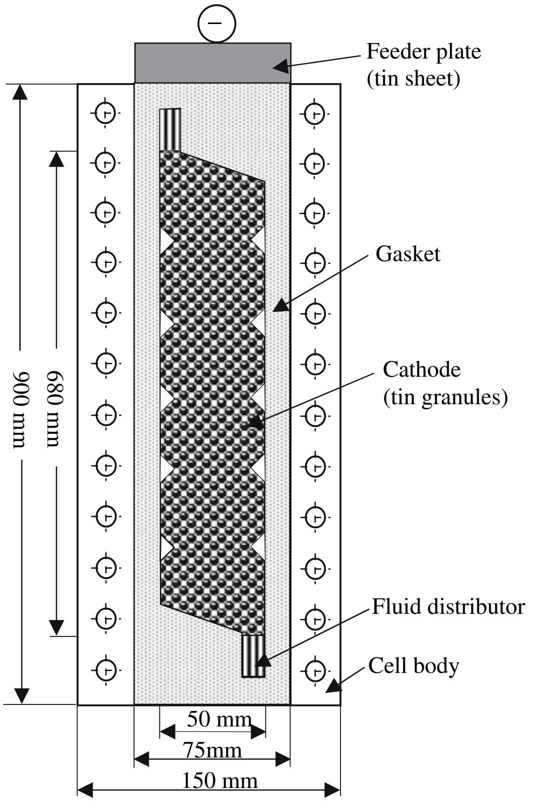

Fig. 2 Front view and dimensions of the cathode compartment of the Reactor B

The schematic process flow diagram was the same as that in our previous work [3, 4]. The essential features of this system involve feeding the catholyte liquid and CO_2 gas to a mixing tee from which they proceed together in 2-phase slug flow to make a single pass upward through the cathode bed. The 2-phase flow in the cathode bed is typically in the gas-continuous to slug flow regime, analogous to that in a trickle-bed thermochemical reactor [8], with the overall pattern approaching plug flow. The anolyte is recycled upward through the anode chamber from a feed tank where the oxygen generated at the anode is disengaged. The system is piped and instrumented to measure and/or control the fluid flows, current, reactor voltage, pressures, temperatures, gas composition, etc., as required by the experimental design.

In most runs the catholyte outlet is discharged at atmospheric pressure (ca. 101 kPa(abs) while the anolyte outlet is controlled at about 20 kPa above the catholyte feed pressure to ensure the membrane is pressed against the cathode and thus suppress catholyte by-pass between the membrane and cathode bed. There is no facility in this system for measuring the individual electrode potentials or the current distribution in the reactor.

2.4 Reactor (cathode) model

A crude model was originally set up for the cathode in Reactor A as a differential continuous reactor in isobaric and isothermal operation at steady-state [3]. This basic model assumes that the formate CE is determined by a competition between parallel reactions I and II, in which the primary reaction I proceeds under a CO_2 mass transfer

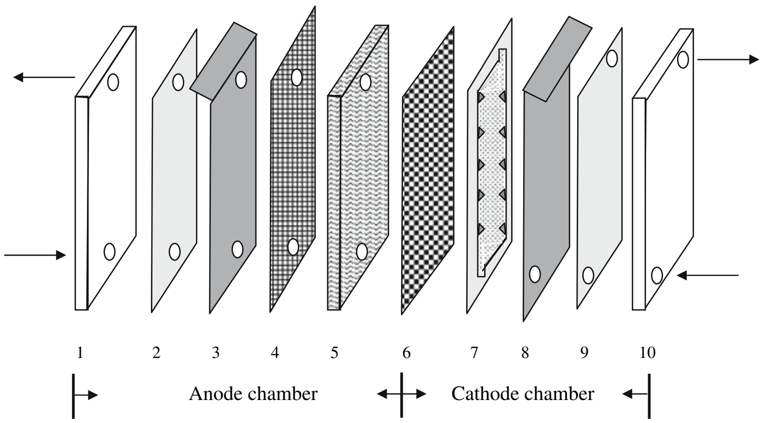

Fig. 3 Reactor configuration. 1 and 10, mild steel cell body; 2 and 9, insulating gaskets; 3, anode current feeder (stainless steel plate); 4, anode mesh (stainless steel mesh); 5, PVC screen anode spacer; 6, Nafion membrane; 7, tin granule cathode contained in Neoprene gasket; 8, cathode current feeder (tin plate)

constraint. In the present work, the model was extended to deal with Reactor B as a plug flow continuous reactor in adiabatic operation at steady-state, with significant gradients in catholyte composition, CO_2 pressure and temperature along the reactor height. Although it is substantial relative to any in the literature on the electro-reduction of CO_2 the model is still primitive, in so far as it does not calculate the potential and current distributions along the cathode height and across the cathode thickness, but instead assumes that the current is distributed uniformly along the cathode height and there is uniform current density on the real surface across the electro-active cathode thickness. The model also assumes zero cross-over of formate from catholyte to anolyte. These assumptions deviate from reality but are considered adequate for the present purposes.

The extended model deals with the intrinsic kinetics of reactions I and II by designating the two rate constants plus two activation energies as adjustable parameters. These four kinetic parameters are fitted (by the method of least squares) to the experimental data from tin granule cathodes in Reactors A and B. Further details on the extended model are presented in the Appendix.

The modeled variations in process conditions along the reactor height under typical operating conditions in Reactor B are shown in Fig. 4 and some model predictions on the effect of superficial current density on formate current efficiency in Reactors A and B are compared to the measured values in Fig. 7 below.

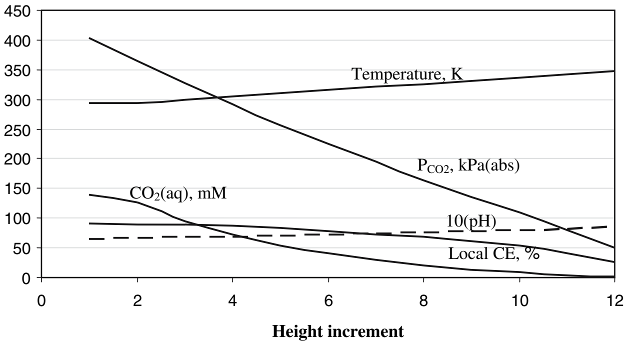

Fig. 4 Modeled local profiles of process conditions for Reactor B at 100 A. Left ordinate scale corresponds to units on each line

3 Results and discussion

3.1 Reactor A

3.1.1 Cathode stability

Exploratory runs on catalytic stability of particulate tin for electro-reduction of CO_2 were carried out in Reactor A for up to 250 min (∼4 h) at 6 A (1.33 kA m^{-2}) with the experimental results presented in Fig. 5. The formate current efficiency (CE) with tin shot (Fig. 5a) showed an initial increase and then stabilized within the tested period (3 h); the formate CE with tin granules (Fig. 5b and c) also showed an increase within the first 30 min, and then stabilized for about 2 h (plateau) before decreasing. The initial gain of formate CE in both cases might be explained by the further clean-up of the tin surface on the cathode through both the flush of the fluid flow and the polarization,

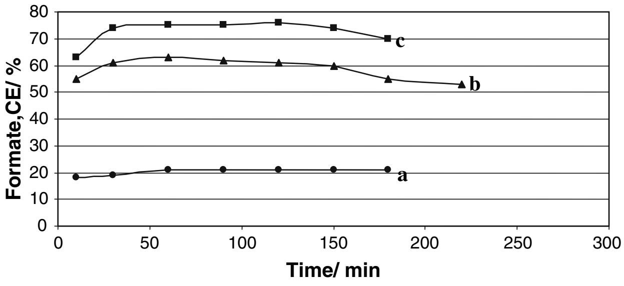

Fig. 5 Formate CE versus cathode age. Reactor A. (a) fresh tin shot; (b) fresh tin granules from Batch 1; (c) fresh tin granules from Batch 2. Operating conditions: current = 6 A; catholyte = 0.45 M $KHCO_3$ + 2 M KCl; gas flow = 364 mL (STP) min^{-1}; catholyte flow = 20 mL min^{-1}; temperature = 300 K; pressure = 116 kPa(abs) on tin shot and 140–170 kPa(abs) on tin granules

which apparently made the cathode more active. It can also be seen that Batch 1 and Batch 2 tin granules exhibited similar sustainability in formate CE within about 2 h but at different levels, i.e. 64% vs. 76%, and tin shot provided a stable catalytic activity (constant formate CE) within the tested period of time, yet at the lower level of 23%. The differences in formate CEs among tin granules and tin shot were presumably due to the variation in specific surface area of granules and tin shot, i.e. respectively, 11,000 and 17,000 vs. 1,500 m^2 m^{-3}, possibly combined with the higher CO_2 pressure in the granule cathodes.

The impurity analyses given in Table 2 show that the level of [Sb, As, Cu and Fe] was much higher in tin granules than in tin shot, which suggests that those impurities might be accumulating at the granule surface and poisoning the cathode as the electro-reduction of CO_2 was proceeding. Two ways of re-activating the deteriorating cathode were investigated: chemical treatment of the cathode and polarity reversal. In the former case, the used granules, after being removed from the reactor, were treated with dilute hydrochloric acid and potassium hydroxide sequentially, washed in water and re-used to run electro-reduction of CO_2. In the latter case, polarity reversal was applied for 5 min at 1 A on tin granules in the course of electro-reduction of CO_2 when the formate current efficiency had dropped from about 70% to 50% after 6 h operation. Both chemical treatment and polarity reversal brought the formate CE back to its initial value of about 70%, thus supporting the hypothesis that accumulation of impurities (e.g. As, Fe) on the cathode surface causes a shift in reaction selectivity in favor of reaction II with increasing operating time.

Compared to the tin-coated copper mesh cathode used in our previous work, for which the formate CE dropped from about 50% to 20% in 100 min [3], tin particles exhibited relatively long and stable operating times (200 min), which is encouraging in terms of the potential industrial development of electro-reduction of CO_2. In the present work, tin granules have been used in the subsequent investigations of process variables and reactor scale-up.

3.1.2 *Reactor A. Process variables with tin granule cathode*

Our previous communications reported the effects of several process variables on the performance of Reactor A with tinned-copper mesh cathodes [3, 4]. The present work was aimed to confirm some of those effects in a tin granule cathode and to extend the data to include the effects of gas and liquid loads in the cathode bed, which are critical to the reactor scale-up. Two sets of factorial experiments [9, 10], along the lines of those in references 3 and 4, were carried out here in Reactor A. The conditions of these experiments and significant effects for the formate current efficiency (CE %) are summarized in Table 3.

The formate CE measured in Experiment (i) ranged from 64% to 87%, with a center-point at 75%. The variation in outlet pH (7.5–7.8) is relatively small and probably has little effect on the reactor performance here. Both current and temperature had significant negative main effects on formate CE, and this result is consistent with that from our previous work with tinned-copper mesh cathodes [3, 4]. On the other hand, both the catholyte (liquid) and gas flow rate had significant positive main effects on formate CE, presumably due to the positive effect of increasing fluid loads on the CO_2 mass transfer capacity of the cathode, together with the increased liquid hold-up and effective ionic conductivity in the 3D cathode that resulted from an increased liquid load [8]. Further, increasing the

Table 3 Factorial experiments with tin granule cathodes in Reactor A

Experiment	Variables and levels	Significant effects @ 95% confidence (% CE)	
		Main	2-Factor
(i) Fractional factorial	C = KCl concentration [0.5–2 M]	–	CG (2.1)
5 variables	G = Gas flow [400–1600 mL STP min^{-1}]	G (+6.2)	GL (−2.2)
V resolution	I = Current [2–8 A]	I (−3.7)	GI (+2.9)
$2^{(k-1)}$ + center-point replicates	L = Catholyte flow [10–20 mL min^{-1}]	L (+2.7)	IL (+4.2)
	T = Temperature [293–323 K]	T (−8.5)	IT (+3.4)
(ii) Full factorial	C = Concentration of KCl [0.5–2 M]	–	
3 variables	I = Current [2–14 A]	I (−42)	IL (−9.8)
$2^{(k)}$ + center-point replicates	L = Catholyte flow [10–20 mL min^{-1}]	L (+14)	

Operating conditions: Reactor A. Batch 2 tin granules. Catholyte = 0.45 M $KHCO_3$ + KCl

(i) Pressure in/out = (136–241)/101 kPa(abs); catholyte outlet pH = 7.5–7.8

(ii) Gas flow = 400 mL (STP) min^{-1}; pressure in/out = (181–231)/101 kPa(abs); temperature = 323 K; catholyte outlet pH = 7.54–9.22

gas flow from 400 to 1,600 mL STP min^{-1} pushed the inlet pressure up by about 65 kPa on average, and this increase in reactor pressure would have a significant positive effect on the CO_2 solubility and mass transfer limiting current density. The main effect of gas load on the reactor (full-cell) voltage in the runs of Table 3 was calculated from the factorial voltage measurements as 0.1 V. This relatively low effect of gas load may occur because the decrease in liquid hold-up and effective catholyte conductivity caused by increasing gas load is partly compensated by corresponding increases in cathode pressure and the CO_2 ($G \rightarrow L \rightarrow S$) mass transfer capacity [5, 8]. The fact that KCl concentration had no significant overall effect on the formate CE corresponds to our previous observations on the effects of catholyte conductivity [4].

In Experiment (ii) the current was taken to an extreme high level of 14 A (3.1 kA m^{-2}) to force the process into mass transfer control. Here the formate CE ranged from 38% to 95%, with strong main effects of I and L (respectively negative and positive), consistent with the expected CO_2 mass transport constraints. The significant two-factor interactions in Table 3 reflect the complexity of this process with respect to the counteracting effects of the main variables on the formate CE, as previously observed [4] and outlined in the reactor model. For example, the sign reversal of the IL interaction from Experiment (i) to Experiment (ii) may be explained by the fact that the 14 A runs in Experiment (ii) (all at G = 400 mL STP min^{-1}) were well into the regime of CO_2 mass transport control, and not compensated by the rise in mass transport capacity due to increasing the catholyte flow from 10 to 20 mL min^{-1}.

3.2 Reactor B

Reactor B was tested as a scaled-up version of Reactor A, to increase the CO_2 conversion and product formate concentration, as well as to substantiate the model and to see the prospects for developing of the reactor to industrial scale. A range of parametric experiments was carried out to examine the cathode stability, together with the effects of current density and formate concentration on reactor performance.

3.2.1 Cathode stability

Figure 6 shows the result of a preliminary trial carried out to check the operational stability of Reactor B in the time frame of the bench scale experiments. Although the operating conditions were nominally held constant here, both the catholyte outlet temperature and inlet pressure increased over the duration of the run, as given under Fig. 6. The rise in temperature is due to the thermal inertia of the reactor, which takes about 1 h to reach a steady-state temperature. The rise in pressure is more problematic and is apparently due to the fact that the cathode for this run was pretreated with nitric acid. This pretreatment leads to the generation of solid corrosion products of tin (mentioned earlier) that may be responsible for slowly plugging the fixed bed cathode. Both the experiments on Reactor A and the reactor model show that formate CE decreases with increasing temperature and increases with increasing CO_2 pressure. The results of Fig. 6 indicate that these effects probably interact with the cathode deactivation (cf. Fig. 5) to stabilize formate CE over the 3.4 h operating period at 96 A.

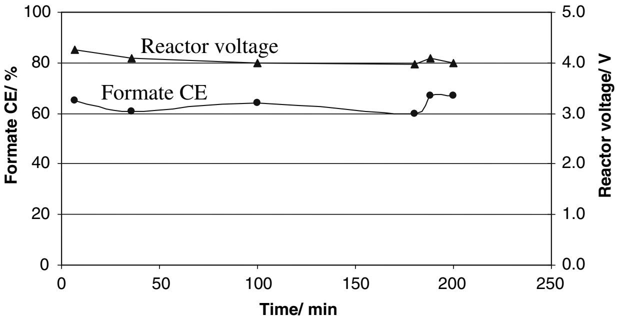

Fig. 6 Operational stability of Reactor B. Operating conditions: Reactor B. Batch 2 tin granules, catholyte = 0.45 M $KHCO_3$ + 2 M KCl; catholyte flow in/out = 20/22 mL min^{-1}, gas flow in = 2,200 mL (STP) min^{-1}; temperature in/(out) = 289/(305–322) K; pressure (in)/out = (400–510)/101 kPa(abs), current = 96 A (3.0 kA m^{-2})

3.2.2 Current density

Table 4 lists experimental data from Reactor B over a range of current densities with runs from 7 to 100 min duration, each of which used newly pretreated cathode granules. Values from Table 4 are plotted in Fig. 7 to compare the effect of superficial current density on formate CE in Reactor A against Reactor B, along with the modeled values of formate CE. Figure 8 shows the corresponding experimental values of the specific energy and formate product concentration in Reactor B. In Fig. 7 the low value of the modeled CE relative to the measured value for Reactor A at 0.45 kA m^{-2} (ca. 85% vs. 95%) may be due to a bias in the kinetic parameters of Table A1 that favors the high inlet CO_2 pressure regime of Reactor B over that of Reactor A (ca. 450 vs. 210 kPa(abs)).

Compared to Reactor A, Reactor B gives substantially higher values of formate product concentration, inlet pressure, temperature rise and outlet pH, e.g. respectively (0.1 vs. 1 M), (200 vs. 600 kPa(abs)), (5 vs. 40 K) and (7.8 vs. 9.6). These differences are mainly due to the predicable effects of scaling up the reactor dimensions (especially the height) and total

Table 4 Effect of superficial current density in Reactor B

Current (A)	20	40	51	88	91	94	100
CD (kA m^{-2})	0.6	1.2	1.6	2.7	2.8	2.9	3.1
Formate CE (%)	91	86	83	67	65	64	63
Operating time (min)	60	80	30	35	7	100	17
[HCOO$^-$] (M)	0.28	0.54	0.64	0.90	0.92	0.94	1.03
Cell voltage (V)	2.70	3.40	3.10	4.30	4.25	4.10	3.90
T (out) (K)	293	296	299	308	305	322	314
P_{cathode}(in) (kPa(abs))	690	690	620	500	500	540	600
Catholyte pH (out)	8.10	8.20	8.16	9.29	9.46	9.47	9.56

Operating conditions: Reactor B. Batch 2 tin granules, catholyte = 0.45 M KHCO$_3$ + 2 M KCl; catholyte flow in = 20 mL min^{-1}; gas flow in = 1,600–2,200 mL STP min^{-1}; CO$_2$ in = 100 vol%; inlet pH = 7.50; outlet pressure = 101 kPa(abs); inlet temperature = 291 K

CD = superficial current density; CE = current efficiency

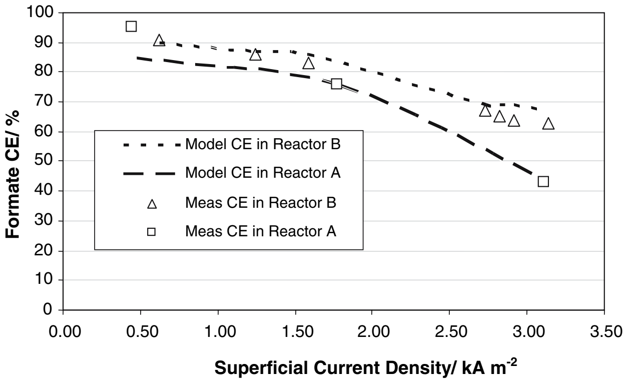

Fig. 7 Comparison of experimental and modeled results in Reactors A and B. Operating conditions: Batch 2 tin granules, catholyte in = 0.45 M KHCO$_3$ + 2 M KCl; CO$_2$ in = 100 vol%. Reactor A: Catholyte flow in = 20 mL min^{-1}; gas flow in = 400 mL STP min^{-1}; temperature (out) = 323 K; pressure (in) = 210–215 kPa(abs), anolyte = 1 M KOH at 30 mL min^{-1}. Reactor B: Catholyte flow in = 20 mL min^{-1}; gas flow in = 1,600–2,200 mL STP min^{-1}; pressure (in) = 420–470 kPa(abs); temperature (out) = 293–322 K, anolyte = 2 M KOH at 60 mL min^{-1}. Note: 3.1 kA m^{-2} ≡ 14 A for Reactor A, 100 A for Reactor B

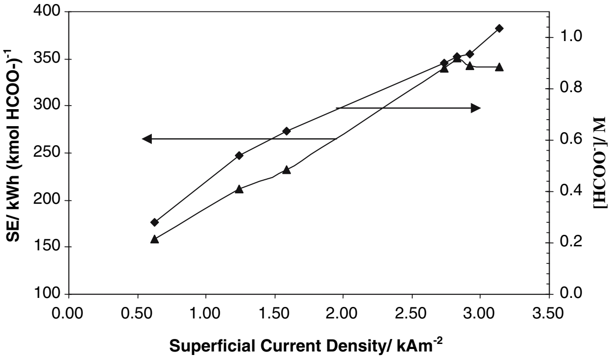

Fig. 8 Effect of superficial current density on specific electrochemical energy and formate concentration in Reactor B. Operating conditions: As under Fig. 7

current relative to the catholyte flow rate. Apart from the consequences of higher pressure and temperature (discussed above) the increased pH can reduce the formate CE by sequestering the electro-active species CO$_2$(aq) into the CO$_2$/HCO$_3^-$/CO$_3^-$ equilibria and shifting the process selectivity to favor reaction II. This effect probably becomes significant at pH above about 9, especially since the local pH at the cathode surface would be about 0.5 units higher than that of the bulk catholyte pH [6, 11].

Figure 7 also shows that at superficial current densities above about 1 kA m^{-2} the formate current efficiency in Reactor B is higher than that in Reactor A. This difference can be explained by the positive effect of the higher pressure in Reactor B on the CO$_2$ solubility and mass transfer limited current density, which shifts the reaction selectivity to favor reaction I. As indicated in Fig. 7 the various effects of current density, flow rates, pressure, temperature and pH in both Reactors A and B are reasonably embraced by the reactor model.

Figure 8 shows that the specific energy for formate increased with superficial current density, reaching about 340 kWh kmol^{-1} formate at 100 A (ca. 3.1 kA m^{-2}). The highest formate concentration obtained in the catholyte product was 1.03 M. This formate concentration is a notable and unprecedented result from a single pass of catholyte through a continuous electrochemical reactor, with a residence time of about 2 min. In comparison Udupa et al. [12] achieved ca. 3 M sodium formate over a 6 h operating period in a CO$_2$ sparged batch reactor with a cation membrane and rotating amalgamated copper (2D) cathode at 0.2 kA m^{-2}. As noted by those authors in 1971 "this method appears to hold good promise for a direct electrochemical reduction of carbon dioxide to (formic acid)". The development of a continuous reactor along the lines described in the present work may make such a process feasible.

3.2.3 *Formate concentration*

A potential industrial process for electro-reduction of CO_2 may involve recycling the catholyte product solution to achieve a high steady-state concentration of primary product formate (possibly as high as 5 M) to reduce the cost of energy and equipment for the separation of formate from the catholyte. To investigate whether a high concentration of formate in the catholyte would adversely affect the performance of the process, single-pass experiments were carried out in Reactor B with formate feed concentration ranging from 0.66 to 3.42 M. Table 5 gives the results for some of these preliminary "recycle" runs. It is seen that as the formate concentration in the feed increased from 0.66 M (run No. 1) to 2.79 M (run No. 4), the formate current efficiency at 50 A dropped from 75% to 36%. The decrease of formate current efficiency with increasing formate concentration could be due to any or all of the following reasons: (1) formate was electro-chemically reduced to other species (such as methanol or formaldehyde) that might not be detected or detected but at a different stoichiometry than formate by the permanganate titration technique, so that the current efficiency was underestimated; (2) formate crossed the membrane to the anode side to be partly oxidized to CO_2, which reacted with OH^- to generate CO_3^{2-}/HCO_3^-; (3) formate accelerated the deterioration of the tin cathode by forming complexes [13, 14] that changed the surface state of the cathode or adversely affected the adsorption of intermediate species involved in the reduction of CO_2. To find which of the three mechanisms accounted for the dropping formate current efficiency, an experiment without CO_2 was carried out (run No. 5) in which N_2 gas was used to duplicate the reactor pressure and flow regime. The catholyte product analysis showed a negative formate current efficiency (−13%), which indicated the possibility of both formate reduction and formate cross-over. Also, the catholyte product from run No. 4 was analyzed for methanol with GC (FID detector, DB-Wax column, <50 ppm) and formaldehyde with HPLC (<5 ppm), from which no methanol or formaldehyde were detected, thus excluding the possibility of formate reduction.

Table 5 "Recycle" runs in Reactor B

Run No.	$[HCOO^-]$ (M) Inlet	$[HCOO^-]$ (M) Outlet	pH out	Gas feed	Formate CE (%)
1	0.66	1.30	9.25	CO_2	75
2	1.44	1.80	9.39	CO_2	44
3	2.12	2.44	9.38	CO_2	44
4	2.79	2.95	9.22	CO_2	36
5	1.55	1.44	9.68	N_2	−13

Operating conditions: Reactor B, Batch 2 tin granules, current = 50 A; catholyte = 0.45 M 0.45 M $KHCO_3 + HCOO^-$; catholyte flow = 20 mL min^{-1}; gas flow = 1,000 mL STP min^{-1}; operating time: 20–330 min; temperature = 291–305 K; pressure = 510–630 kPa(abs)

Table 6 "Recycle" runs with carbon balance in Reactor B

Run No.	Current (A)	$[HCOO^-]$ in feed (M)	Formate CE on cathode side (%)	Formate CE on anode side (%)	Real CE (%)
1	40	2.57	26	59	85
2	20	3.42	−26	117	91

Operating conditions: as under Table 5

The transport of formate through the membrane was confirmed by further experiments in which the anolyte product was analyzed for both formate and bicarbonate/carbonate to see how much of the formate current efficiency was lost due to cross-over of formate. Experimental results are listed in Table 6, in which the formate current efficiency on the cathode side ("apparent" formate CE) was measured by the difference of formate concentrations between the inlet and outlet of the catholyte while the formate equivalent CE on the anode was calculated by the amount of formate and bicarbonate/carbonate in the anolyte due to formate cross-over (i.e. a carbon balance). The "real" formate CE was the sum of the cathode side formate CE and anode side formate CE. Table 6 shows that the "apparent" CEs were significantly lower than the "real" CEs, which match those obtained with zero feed formate (Fig. 7). Such results indicate a problem with formate cross-over in the Nafion 117 membrane that must be confronted in future work on this process.

4 Conclusions

The electro-reduction of carbon dioxide to potassium formate has been scaled-up in the laboratory from a small (A: 45×10^{-4} m^2) to a large (B: 320×10^{-4} m^2) single-cell reactor, operating in the continuous "trickle-bed" mode with co-current 2-phase flow of catholyte liquid and CO_2 gas. Good performance was obtained in both reactors using tin granule cathodes in experiments ranging from 2 to 100 A. The temporal stability of particulate tin cathodes was substantially better than that of the tinned-copper mesh cathodes previously reported [3, 4] (i.e. 200 vs. 20 min) and appears to be limited by accumulation of impurities on the tin surface—although the possibility of slow loss of tin by corrosion should not be discounted.

Experimental results from Reactor A confirm previous conclusions on the effects of process variables [4] and further show positive effects of cathode liquid and gas loads on the formate CE, which are attributed to increasing the CO_2 mass transfer capacity of the 3D electrode. The effect of the gas load on the reactor voltage is relatively small (i.e. ±0.1 V). The seven-fold scale-up Reactor B gave analogous performance to that of Reactor A, with an increase in product formate concentration, pressure drop, pH and temperature rise, as predicted by a crude four parameter model of the cathode processes based on the assumption of parallel reactions for the electro-reduction of CO_2 to formate and of water to hydrogen.

Operating with inlet CO_2 pressures up to 600 kPa(abs) and outlet temperature up to 325 K, using a catholyte and anolyte, respectively [0.5 M $KHCO_3$ + 2 M KCl] and 2 M KOH, Reactor B gave formate current efficiency from 91% to 63%, corresponding to superficial current density of 0.62–3.1 kA m^{-2} (20–100 A), under the same range of reactor voltages (2.7–4.3 V) as that in Reactor A. At 3.1 kA m^{-2} a formate product concentration of 1 M was obtained in a single pass through the Reactor B, with 63% current efficiency and specific energy of 340 kWh per kmol formate. However, results from a catholyte feed spiked with 2–3 M potassium formate indicated significant cross-over of formate through the Nafion 117 membrane. Future work here should be aimed at increasing the cathode life, reducing formate cross-over and optimizing the reactor with respect to its use in processes for the electro-synthesis of formate/formic acid.

Acknowledgement This work was funded by the Natural Sciences and Engineering Research Council of Canada (NSERC) and supported by the University of British Columbia.

5 Appendix

5.1 Extended reactor (cathode) model [6]

The extended model divides the plug flow tin granule (3D) cathode into N increments of height and calculates the overall performance at steady-state by forward differencing in an Excel spreadsheet. In each height increment the model involves relationships for the stoichiometry, equilibria and kinetics of the electro-chemical reactions, including mass transfer of the CO_2, as detailed in previous communications [3, 5]. In the extended model, changing conditions along the reactor height are handled with extra equations involving the thermo-chemical kinetics, electrolyte conductivity, CO_2 solubility, transport properties, etc., that are used to solve the (steady-state) material and energy balances for the CO_2 partial pressure, $CO_2(aq)$ concentration, formate concentration, pH, temperature and current efficiency profiles up the cathode, such as those shown in Fig. 4.

The extended model does not assume CO_2 equilibrium between gas and liquid but instead calculates the concentration of $CO_2(aq)$ in the bulk catholyte as a dynamic variable that depends on the relative rates of mass transfer, thermo-chemical reaction and electro-chemical reaction of CO_2. The superficial current density is assumed uniformly distributed along the reactor height and the local current density is assumed uniform across the electro-active bed thickness. Formate cross-over from catholyte to anolyte is taken as zero and the reactor is assumed to operate under adiabatic conditions, with no resistance to heat transfer between catholyte and anolyte. The model deals with the intrinsic kinetics of reactions I and II by designating the two rate constants plus two activation energies as adjustable parameters that are fitted to the experimental data as outlined below.

The extended model formulates the reaction kinetics as a function of $CO_2(aq)$ concentration, cathode potential and temperature, i.e. for the reactions:

E^0 V (SHE) @ 298 K, pH 14

$$CO_2(aq) + H_2O + 2e^- \rightarrow HCOO^- + OH^- \quad -1.02 \qquad (I)$$

$$2H_2O + 2e^- \rightarrow H_2 + 2OH^- \quad -0.83 \qquad (II)$$

Assuming the intrinsic kinetics of both reactions I and II fit the Tafel form with reaction I under a CO_2 mass transfer constraint, the individual over-potentials are related to the partial real current densities by:

$$\eta_1 = E - E_{r,1} = a_1 - b_1 \log(j_1) + b_1 \log(1 - j_1/j_{1L}) \qquad (1)$$

$$\eta_2 = E - E_{r,2} = a_2 - b_2 \log(j_2) \qquad (2)$$

The Tafel equations 1 and 2 were originally set up with Sn and Cu for the tinned-copper mesh cathode in Reactor A, in which the tin coverage decreased with operating time [3]. Modeling Reactor A and B with a tin granule cathode assumes a fixed tin surface (i.e. tin coverage = 100%) and so does not use the kinetics on copper. The Tafel slopes of both reactions I and II were assumed as 0.118 V/decade at 298 K [15, 16], with a charge transfer coefficient of 0.5, and corrected for temperature by:

$$b = \frac{2.303RT}{\alpha F} \qquad (3)$$

in which: α = electro-chemical charge transfer coefficient = 0.5 (assumed).

The Tafel constants and their temperature dependence involve four parameters that were fitted in the model from experimental data. First, the exchange current densities are calculated from:

$$i_{o,1} = 2Fk_1[\mathrm{CO_2(aq)}]\exp\left(-\frac{E_{a,1}}{RT}\right)\exp\left(-\frac{\alpha_1 FE_{r,1}}{RT}\right) \quad (4)$$

$$i_{o,2} = 2Fk_2\exp\left(-\frac{E_{a,2}}{RT}\right)\exp\left(-\frac{\alpha_2 FE_{r,2}}{RT}\right) \quad (5)$$

Then the Tafel constants are obtained as:

$$a_1 = \left(\frac{RT}{\alpha_1 F}\right)\ln(i_{o,1}) \quad (6)$$

$$a_2 = \left(\frac{RT}{\alpha_2 F}\right)\ln(i_{o,2}) \quad (7)$$

with $\alpha_1 = \alpha_2 = 0.5$ (assumed).

The electrochemical kinetic parameters k_1, k_2, $E_{a,1}$ and $E_{a,2}$ were fitted in the model from the experimental data—with the constraint that the values of $i_{o,2}$ and a_2 should approximate those found in the literature e.g. respectively about 1×10^{-7} kA m^{-2} and -0.8 V on Sn at 298 K [16, 17]. The activation energies were also kept within the typical range of electrode reactions i.e. about 30×10^3–100×10^3 kJ kmol^{-1} [17].

Figure A1 shows a parity graph of modeled versus measured values of the formate CE for the range of process conditions outlined in Sect. 3 above. The line of best fit, obtained by the method of least squares, has a slope of 1.01, regression coefficient (R^2) of 0.64 and maximum error of about ±20%. These results give some support to the model, while pointing to the need for more work in this area. The corresponding fitted values of the kinetic parameters are given in Table A1 and reflect the relatively slow kinetics and weak effect of temperature for reaction II versus reaction I on a tin cathode.

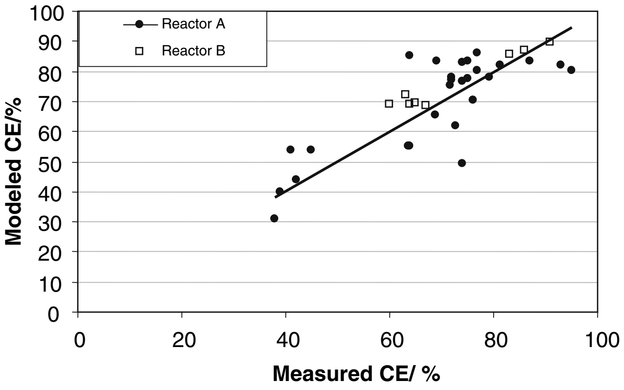

Fig. A1 Modeled versus measured formate CE for tin granule cathodes in Reactors A & B. Replicate runs excluded

Table A1 Parameter values for best fit of modeled and measured formate CE

Parameter	k_1 (m s^{-1})	k_2 (m s^{-1})	$E_{a,1}$ (kJ kmol^{-1})	$E_{a,2}$ (kJ kmol^{-1})
Value	55×10^{-5}	45×10^{-12}	60×10^3	32×10^3

References

1. Chaplin RPS, Wragg AA (2003) J Appl Electrochem 33:1107
2. Schibioh MA, Viswanathan B (2005) Proc Indian Natl Sci Acad 70A(3):407
3. Li H, Oloman C (2005) J Appl Electrochem 35:955
4. Li H, Oloman C (2006) J Appl Electrochem 36:1105
5. Oloman C (1979) J Electrochem Soc 126:1885
6. Li H (2006) Development of a continuous reactor for the electrochemical reduction of carbon dioxide, Ph.D. Thesis. Department of Chemical and Biological Engineering, University of British Columbia
7. Goodridge F, Scott K (1995) Electrochemical process engineering: a guide to the design of electrolytic plant. Plenum Press, New York and London
8. Hodgson I, Oloman C (1999) Chem Eng Sci 54:5777
9. Box GEP, Hunter JS (1961) Technometrics 3(3):311
10. Murphy TD (1977) Chem Eng 6:168
11. Gupta N, Gattrell M, Macdougal B (2006) J Appl Electrochem 36:161
12. Udupa KS, Subramanian GS, Udupa HVK (1971) Electrochim Acta 16:1593
13. Sillen LG, Martel AE (1964) Stability constants of metal ion complexes. Chem. Soc., London, Special publication 17
14. Pourbaix M (1974) Atlas of electrochemical equilibria in aqueous solutions. NACE, Houston, p 475
15. Vassiliev Y, Bagotzky V, Oseterova N, Khazota O, Mayorova N (1985) J Electroanal Chem 189:271
16. Pickett D (1977) Electrochemical reactor design. Elsevier, Amsterdam
17. Conway B (1952) Electrochemical data. Elsevier, London